ORIGINAL ARTICLE

The large deep-seated landslide induced by the March 12th, 2012 rainfall event in the city of Azazga, Northern Algeria: deformation characteristics and failure mechanisms

Hamid Bourenane[1] · Rabah Bensalem[1] · El Hadi Oubaiche[1] · Massinissa Braham[1] · Aghiles Abdelghani Meziani[1] · Youcef Bouhadad[1] · Mohamed Yacine Tebbouche[1]

Abstract

A rainfall-induced deep large landslide occurred on March 12, 2012, in the city of Azazga (Northern Algeria), causing heavy damages to residential buildings and public infrastructures. In this work, we investigate the inventory mapping, the deformation characteristics, the controlling factors, and the failure mechanisms of this landslide based on the field investigation, aerial photographs and satellite images interpretation, deep boreholes equipped with piezometers and inclinometers, as well as subsurface geophysical imaging by electric resistivity tomography (ERT). The obtained landslide inventory map shows that the landslide of March 2012 affected an area of 0.40 km². This landslide is considered as a partial reactivation of a large pre-existing one (0.606 km²), which represents 6.65% of the total urban area. Moreover, the analyses identified two types of causative factors: (1) the triggering factor related to the high intensity and antecedent rainfall as well as human activity through slope excavations and embankments; and (2) the susceptibility factors related to the lithological nature and the internal structure of the flysch deposits, their weak mechanical resistance characteristics, the presence of shallow aquifers, and basal undercutting erosion of the Iazoughen and Aboud river torrents. The inclinometer measurements and ERT imaging reveal a complex, deep-seated and rapidly moving landslide whose failure surfaces are located at a depth of 11–29 m with an average velocity of 1–29 cm year⁻¹. The entire slip surface is located along the geotechnical interface between the flysch bedrock and the overlying scree. This comprehensive study provides useful information on rainfall-induced landslides and may constitute guidance for landslide hazard mitigation and prevention.

Keywords Deformation · Mechanism · Rainfall · Field investigations · Inclinometers · ERT · Azazga (Algeria)

Introduction

Rainfall-induced landslides are among the most recurrent and damaging geological hazards that cause substantial negative consequences in the north of Algeria, especially in urban areas. They constitute a serious threat to human lives and their properties and a major constraint on the economic development and urban planning of many cities in the country (Bourenane et al. 2014; 2016).

The city of Azazga, situated in the mountainous province of Grande Kabylia in the north of Algeria, is one of the most affected urban areas by recurrent and widespread landslides (Djerbal et al. 2012; Bourenane et al. 2021a, b). The occurrence and frequency of landslides are related to the interaction between the natural susceptibility factors (geological structures, the mechanical properties of the bedrock, the local geomorphic and the tectonic controls) and the triggering mechanisms (rainfall intensity, snow melting and human activity). Therefore, the deformation mechanisms of rainfall-induced landslides are complex due to several geomorphological and climatic settings as well as human activities.

The active landslides of Azazga city are alarming because of their localization in urban environment with a high density of population, their great extension and the serious damage they cause to dwellings and public infrastructure. The landslide occurrence has been largely triggered by

✉ Hamid Bourenane
  b.hamid725@gmail.com; b.hamid@hotmail.com

[1] Division Microzonage Sismique, Centre National de Recherche Appliquée en Génie Parasismique (CGS), 1 Rue Kaddour Rahim, Hussein Dey, Algeria

frequent extreme rainfall events during the rainy season (CGS 2018; Bourenane et al. 2021a, b). The most historical cases occurred in 1952, 1955, 1973, 1974, 1984, 2003, 2004, 2012, 2014, 2018 and 2019 (Bourenane et al. 2021a, b), which were caused and reactivated by intense rainfall during the winter season, causing substantial damage to several constructions, roads and infrastructures in diverse districts of the urban area.

The heavy rainfall and snowfall of March 2012 triggered and reactivated various types of landslides, such as rock falls, rockslides, debris slides and debris flows within several sites of the urban area of Azazga, such as Tala Oukouchah, Zen, Ighil Bouzel, Agouni Guizem and Aït Bouhouni (Fig. 1). The slope movements have caused damage to roads, settlements of houses and public infrastructures over an area of about 2 km² (Fig. 2a).

The Ighil Bouzel landslide is one of the most complex, damaging and the largest active landslides that affected the vicinity of Ighil Bouzel village, north of the city of Azazga. It occurred on March 12, 2012, at 3:00 am, following the long lasting and intensive rainfall that started in early February. The landslide induced ground deformation was extensively observed in the most susceptible areas around Tala Oukouchah, Zen and Ighil Bouzel villages, mainly along the Iazoughen river, where the geomorphological, geotechnical and hydrogeological conditions are the most favorable. The Ighil Bouzel landslide constitutes a great concern and represents an important risk, and therefore a high-priority scientific challenge, because of its location in urban areas,

its large extension and the extent of the induced disorders. Understanding the characteristics of landslides, as well as their causative mechanisms and evolution, is a real challenge and vitally important for prediction, monitoring and control of landslide occurrences as well as for providing helpful information for choosing landslide hazard mitigation measures (e.g., Dai and Lee 2001, 2002; Chau et al. 2004; Harp et al. 2011; Guzzetti et al. 2012; Bourenane et al. 2016).

Previous geotechnical studies have contributed to the identification of the geological, hydrogeological and geotechnical characteristics of the Ighil Bouzel site (LCTP 2012) and the geometry of the sliding mass (LCTP 2014), revealing the existence of surface discontinuities based on the sounding investigations using both piezometers and inclinometers. Despite the availability of some interesting geotechnical data, the complex structure, deformation characteristics, as well as the causes of the triggering and evolution mechanism of the Ighil-Bouzel landslide remain unknown. Therefore, geomorphological mapping, detailed land investigations and geophysical methods should be very useful in this structural context, particularly when identifying older scarps, which mark different phases of its evolution mechanism, is required because they mark different phases of its evolution. For this purpose, the electrical tomography should be combined and calibrated with the available geotechnical data in order to identify and characterize the internal structures of landslides.

In this study, we present the first complete inventory mapping, deformation characteristics, influencing factors

Fig. 1 Examples of different types of landslides induced by the March 12, 2012 rainfall event in the city of Azazga: **a** debris flow and damage to constructions in Agouni Guizem, southeast of the city, **b** debris flow along the Boulina river, south of the city, **c** damages of municipality road in the Agouni Guizem, **d** damage along national road RN 12 in Ighil Bouzel and Zen, north of the city

Fig. 2 Geographical setting of the study area within: a) the north center of Algeria and at East of the capital city Algiers; **b** administrative limit of the urban perimeter of the city of Azazga and spatial distribution of landslides induced by the 12 March 2012 rainfall event on the digital elevation model (DEM)
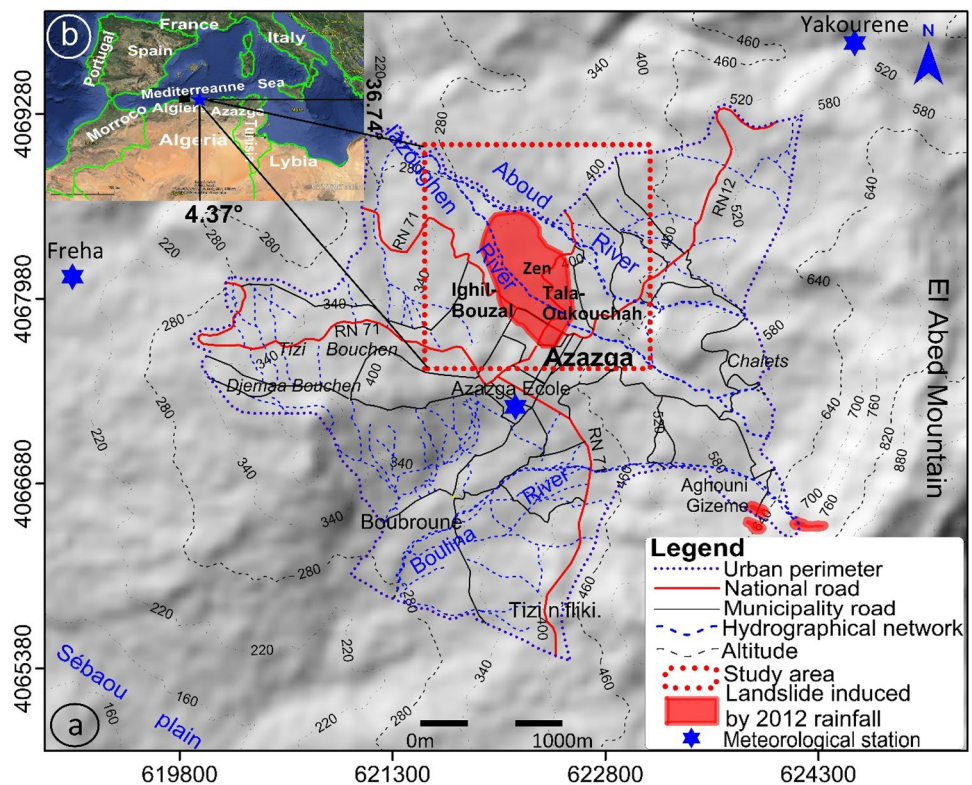
and failure mechanisms of this complex and large rainfall-induced landslide based on the field investigation, aerial photographs/satellite images interpretation, boreholes equipped with piezometers and inclinometers, as well as subsurface geophysical imaging by electric resistivity tomography (ERT). This exhaustive study provides field evidence and methods for the identification and mapping of rainfall-induced complex landslides, as well as guidance for the reduction and prevention of landslide hazard and risk.

Description of the study area

The landslide occurred in Ighil Bouzel village, which is situated in the north of the city of Azazga (Northern Algeria) along the left bank of the Iazoughen river (Fig. 2a), about 135 km east of the Algerian capital, Algiers (Fig. 2b) and about 35 km east of the Tizi Ouzou prefecture (Wilaya). Oriented north-west–south-east, the affected area is an ancient landslide with an extremely wide distribution of surface effects. The unstable site is located within the urban zone perimeter and defined by its geographical coordinates: latitude 36.749° N and longitude 4.371° E. This deep-seated landslide has been known since the 1970s as one of the most active and largest landslide and is still evolving.

Geomorphologically, this important landslide belongs to the massif of Grande Kabylia, in the Northern part of the Tellean Atlas chain. The unstable zone is a hilly area

located on the foothills of the El Abed Mountain with a slope dipping toward the north at an angle of 6°–10° (Fig. 2a). The upper slope part is relatively gentler than the lower one. The landslide head scarp appeared at the market place in the city center near the national road RN 12 at an elevation of 450 m (above sea level) and the landslide toe is at an elevation of 330 m near the converging zone between the Aboud and Iazoughen rivers.

The main geological structure of the area belongs to the North-Kabyle Flyschs domain, located in the internal zones of the Maghrebides chain (Fig. 3). The study area is built on Cretaceous–Oligocene flysch bedrock that consists of thick-bedded complexes of clay and marl formations, largely outcropping on the surface above a thick series of Numidian clays and sandstones, forming the main land-forms to the east and covered by quaternary scree deposits to the north (Gelard1979; ORGM 1996). Tectonically, landslides are located in the flysch area, an allochthonous domain characterized by thrust sheets that have been displaced during or after their sedimentation during the alpine tectonic phase. The main tectonic features include (Gelard 1979; ORGM 1996): (Fig. 3) (1) a major tectonic contact, oriented N–S, separating the "flysch of Azazga" unit and the Numidian unit; (2) A system of faults in two main directions, SW–NE and NW–SE, visible particularly in the Numidian sandstones; and (3) The overthrust of Numidian sandstones onto Cretaceous clay to the west.
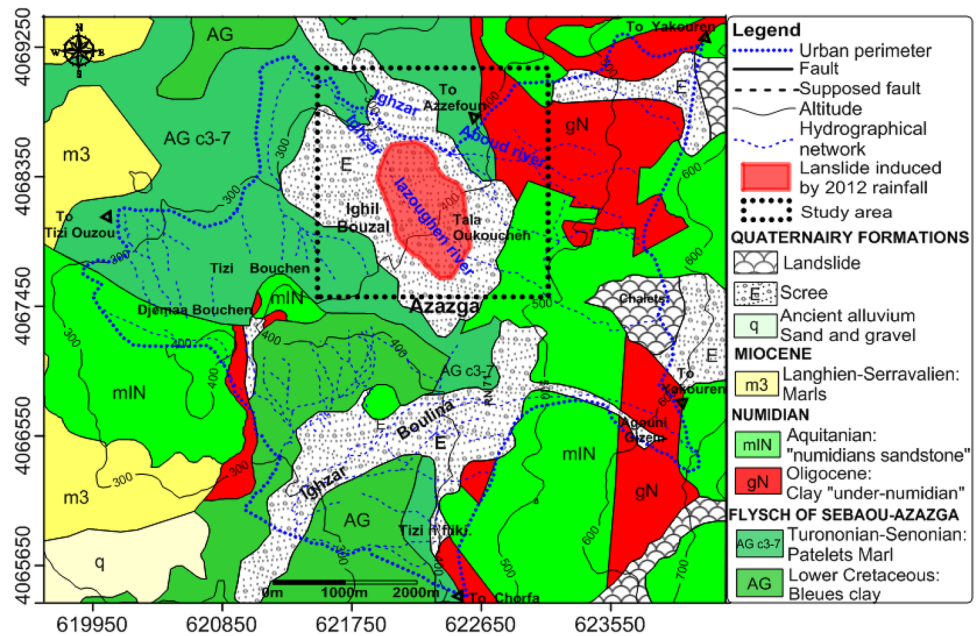
The Azazga region is highly prone to rainfall-induced landslides due to its climatic conditions of "Mediterranean type", characterized by the high intensity of precipitation (700–1200 mm year^{-1}) over a short period during the rainy season extending from December to February that represents 50–60% of the yearly precipitation (Bourenane et al. 2021a, b).

From the hydrological point of view, the NW–SE oriented Aboud and Iazoughen rivers developed on both sides of the landslide with a semi-permanent flow that are associated with the temporary flow of affluent waterways (Fig. 2a). The hydrogeology of the area is largely controlled by the distribution of the permeable quaternary scree and the impermeable flysch stratum of clay and marl (Fig. 3). In addition, the altered and fractured substrate involves a major role of meteorological water infiltration along the main faults and cracks (permeability of cracks), which affects the equilibrium state of the slope and participates in the evolution and speed of sliding.

Data and methodology

Database preparation

In order to investigate in more detail the rainfall-induced landslide on March 12, 2012, the available in situ investigations that include geological, geotechnical and hydrogeological data, carried out by several companies in the framework of construction project studies, have been compiled, analyzed and processed with various techniques. These data were integrated into a GIS database using MS Access and Arc GIS 9 in the same Algerian local projection system (UTM Zone 31 North and WGS 1984; spindle 31 North). The prepared database includes (Fig. 4):

- The rainfall database covers a period of 64 years from the three meteorological stations "Azazga Ecole, Yakourene and Freha" monitored by the National Agency of Water Resources (ANRH 2019). The data set comprises the list of daily, monthly and annually measured rainfall for the period starting from 1950 to 2014. The location of the meteorological stations (rain gauges) is shown in Fig. 2a.
- Geological investigations data of the study area such as lithology, bedrock and tectonic structure obtained from the digitization of the published geological map at a scale of 1:50,000 by the National Office of Geological and Mining Research (ORGM 1996).
- Geotechnical investigations data including nine boreholes of depth ranging between 30 and 36 m among them six equipped with inclinometers (BI), three equipped with piezometers (BP), as well as 20 laboratory tests of selected samples in subsoil layers carried out as part of a geotechnical investigation in the framework of a land use plan study (LCTP 2012) and as a specific geotechnical investigation of the landslide of March 2012 (LCTP 2014).
- Hydrogeological investigations conditions concerning rainfall infiltration mechanisms, groundwater level and their influences on stability through field monitoring programs. The program concerns the inventory of the 65 existing water points (4 springs and 61 wells) throughout the study area for the high-water period (between December and June) conducted by the National Center

Fig. 4 The location of boreholes, inclinometers, water points, cross-sections and ERT profiles
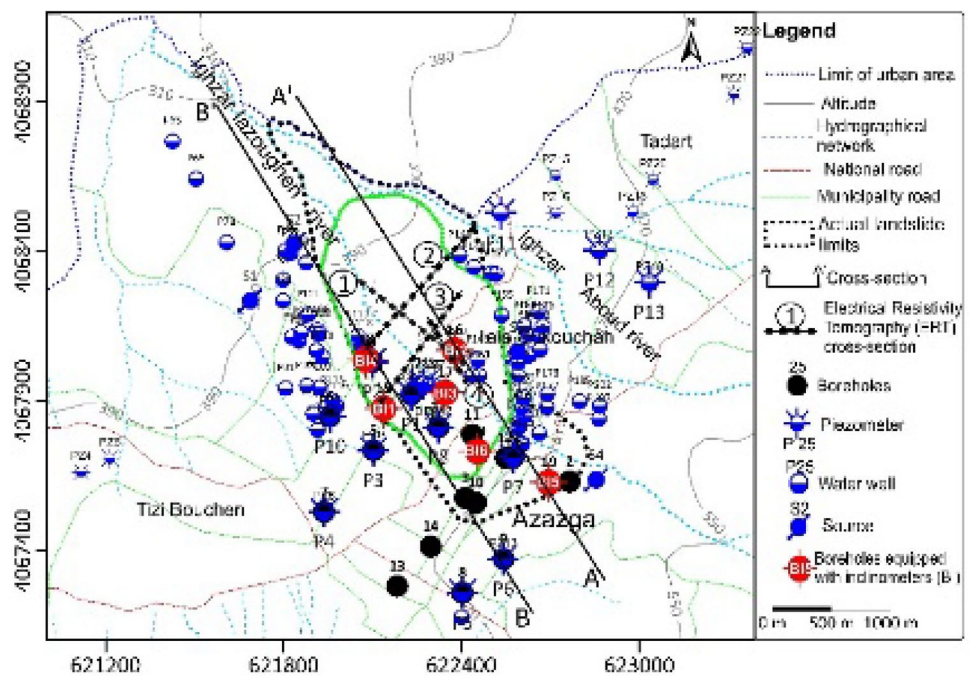
of Applied Research in Earthquake Engineering (CGS 2014).

- The topographic digital data obtained from a digital elevation model (DEM) with a 10 m resolution obtained by the digitization of topographic maps at a scale of 1:25,000 provided by the Institute of Cartography and Remote Sensing (INCT). Then the DEM is used to extract topographical parameters (e.g., elevation and slope gradient) using GIS. The hydrographic network, roads and other basic geographical data were also digitized from the topographic maps, high-resolution satellite imagery Alsat 2A (taken in 2011), completed by our geological fieldwork investigations.

- The geophysical investigation data consists of electrical resistivity tomography (ERT) measurements carried out by CGS in 2020 with the dipole array along four profiles along and across the largest landslide areas.

The locations of boreholes, water points, inclinometers and the positions of cross-sections and ERT profiles are shown in Fig. 4.

Landslide inventory mapping

Following the March 2012 rainfall events, we executed a geomorphological map based on the exhaustive field investigations to identify and map the rainfall-induced landslides. The detailed active landslide is mapped in ArcGIS at a scale of 1:10,000 based on: (1) the analysis and interpretation of black and white aerial photographs at different scales: 1/20,000, 1/10,000 and 1/4,000 taken in 1973, 1984, 2000

and 2008 respectively. These aerial photographs are provided by the Algerian Institute of Cartography and Remote Sensing (INCT); (2) the analysis and interpretation of recent high resolution (2.5 m) Alsat images taken in 2011 by the Algerian Space Agency (ASAL); (3) the analysis of Google Earth satellite images from 2003 to 2012, with a spatial resolution of 15 m; (4) analysis of DEM (10-m resolution) generated by digitizing and kriging interpolation of elevation lines extracted from the topographic maps at a scale of 1:25,000; (5) analysis of archive documents and available data (technical reports of LCTP 2012, 2014; CGS 2010, 2018) and completed by (6) detailed geomorphological field surveys.

Analysis of the deformation characteristics, the landslides controlling factors and the failure mechanisms

To investigate the deformation characteristics, the internal structures, the failure mechanisms and the main controlling factors of the landslides in more detail, we are based on: (1) the analysis of the historical inventory of the landslides; (2) the interpretation of the aerial photographs at scales of 1/20,000, 1/10,000 and 1/4 000, satellite images Alsat 2A with a resolution of 2.5 m, as well as Google Earth satellite images with a resolution of 15 m and (3) analysis of the available geological, hydrogeological, geotechnical and geophysical investigations carried out by several companies in the framework of various studies (LCTP 2012, 2014; CGS 2014, 2020).

The detailed characteristic features of the landslide, including head and side scarps, tension cracks, fissures,

subsidence, bulges and hummocky-shaped areas, are based mainly on field surveys carried out immediately after the rainfall event of March 2012.

The lithological properties of the landslide area, including material structure and thickness of lithological units, are characterized using data from boreholes, which are used to prepare the simplified cross-sections illustrating the lithological structure of the studied area.

The geotechnical properties of the lithological unit are determined based on the analysis and processing of laboratory test data from several geotechnical investigation campaigns carried out in the study area (LCTP 2012, 2014). Ninety undisturbed samples from various depths of lithological unit in the sliding mass were analyzed to measure the grain size distribution (Fc), degree of saturation (Sr), dry unit weight (γd), liquid limit (LL) and plastic limit (PL). In this study, the Atterberg limits (LL and PL) were determined by the Casagrande test (LCTP 2012). The samples for laboratory tests were collected in the landslide area according to the lithological units (Table 1). The geotechnical tests, in accordance with American Society for Testing and Materials (ASTM) standards (Bowles 1992), were performed on undisturbed samples collected from the slopes during the rainy seasons. The average values were separately calculated for each lithology in the laboratory tests. The soil analysis results are given in Table 1.

To investigate the influence of the controlling factors on the occurrence of landslides, rainfall, land use, geology, morphology, hydrogeology and geotechnical characteristics of the soil were examined using in situ investigations of geological, geotechnical and hydrogeological data (boreholes, piezometers, inclinometers, laboratory tests…) carried out by several companies.

In order to better characterize the surface and depth displacements and the failure mechanism of the unstable slope, particularly the depth and the internal structure of slope deformations, we performed inclinometer monitoring measurements and ERT investigations, which were completed by field observation. The results of inclinometeric and ERT investigations are correlated with the boreholes.

Results

## The March 2012 rainfall event

Rainfall is the major triggering factor identified and monitored at the study site. It is known that high-intensity rainfall is a rare event that triggers landslides and induces significant morphological changes in large areas. From early winter of 2011 to early spring of 2012, the Azazga region has been affected by a series of consecutive rain events, defined as a "rainfall event" by a group of rainy days preceded and followed by at least 1 day with no rain (Gullà et al. 2012). Figure 5 shows the rainfall events registered by the Azazga Ecole rain gauge, with indications of the duration (days), the maximum value of daily rainfall (mm) and the cumulated value of rainfall registered in the entire event (mm). On March 12, 2012, a heavy rainstorm triggered several landslides where the registered 24-h rainfall exceeded 19.6 mm. Since January 2012, the estimated precipitations are 262 mm (January), 232 mm (February), 127 mm (March) with 56.5 mm recorded between 1 and 12 March, which are the greatest in the last 20 years. Cumulative peak rainfall over these three months reached 691 mm in 2012, which represents 65% of the annual precipitation (Fig. 5). The rainfall frequency increased from January 12 to March 3, 2012 and the maximum daily rainfall reached over 30 mm. The antecedent rainfall at that time could have been the main factor that induced the failure of the Ighil Bouzel slope. Landslide activity reaches its maximum during and just after rainy events. Considering the series of rainfall data from 1 January 1950 and 12 March 2012, it is possible to know the periods during which the daily rainfall values were higher than those recorded on March 12, 2012. High precipitation on 1–12 March 2012, along with well-saturated soil by antecedent rainfall, led to the development of slope failures.

Table 1 The statistical result of the physical and mechanical parameters of the landslide soil samples

Geotechnical properties	Fc (%)	γd (t/m^3)	Sr (%)	PL	LL	Cc	Cs
Lithology	Min–Max Average	Min–Max Average	Min–Max Average	Min–Max Average	Min–Max Average	Min–Max Average	Min–Max Average
The Cretaceous weathered greenish-grey clays	56–98 82	1.35–1.88 1.61	81.5–100 93.37	20–38 29	48–77 63	12.36–24.21 20.54	2.8–8.9 6.68
Cretaceous compact grey-blue clays	55–100 84.74	1.52–2.02 1.754	37.17–100 89.63	10–33 23	21–69 50	13.81–37.14 20.05	4.09–11.37 7.98
Quaternary screes	15–98 66.35	1.41–1.93 18.537	10.68–100 85.22	7–35 21	23–35 21	5.97–34.54 20.87	1.96–11.74 6.80

Fc: particles size < 0.08 mm, Sr: degree of saturation, γd: dry density. LL: liquid limit, PL: plastic limit, Cuu: unconsolidated and undrained cohesion, φuu: unconsolidated and undrained angles of friction. Min–Max, average are minimum, maximal and average value, respectively

Fig. 5 Daily average and cumulative rainfall from December 1 to 30 of March 2012 at the Azazga Ecole meteorological station of Azazga city. The red star marks when the Ighil Bouzel landslide occurred
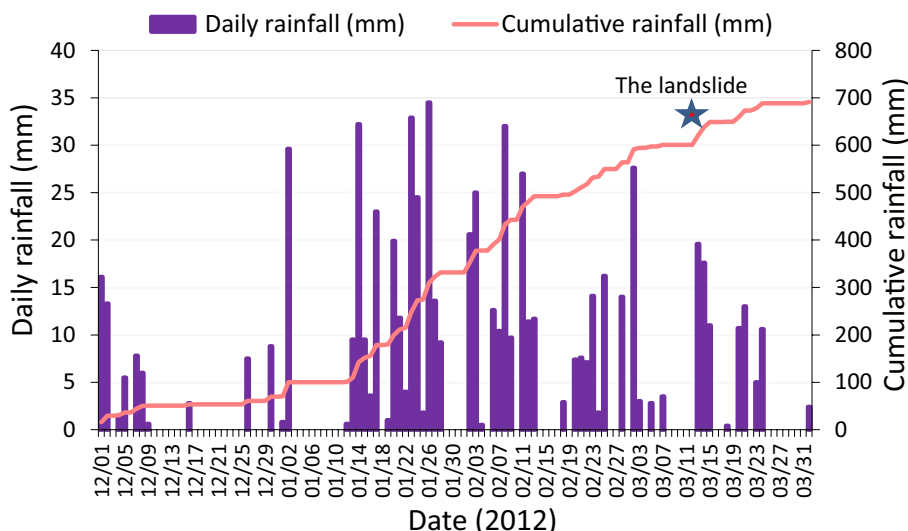

Landslide inventory map

The inventory map of the landslide zone has been prepared at a scale of 1:10,000 and is presented as polygons in Arc GIS. The resultant landslide inventory map is draped over a 10-m resolution ASTER-derived digital elevation model (DEM) and the geology of the study area (Fig. 6). The obtained landslide perimeter of the entire active zone covers an area of 0.606 km^2, which represents 6.65% of the total urban area of Azazga. The boundaries extend over approximately 1570 m in length and a width varying from 350 to 550 m. With a mean depth of 18 m, the estimated surface area of the landslide body is 852.5×10^4 m^2 and the volume is around 153.45×10^5 m^3. According to the classification of Varnes (1978), the majority of the mapped

slope instabilities can be grouped into slide types. These landslides are slow movements that can, under heavy rainfall, evolve into sudden slides recognizable by the formation of head fractures, scarps and dense traction cracks of varying depths and lengths.

The Ighil Bouzel mass movements induced by March 12, 2012 mainly affect the scree over a length of 1000 m and a width of 550 m, covering an area of 550×10^3 m^2. Considering the mean depth of 18 m, the evaluated surface area of the landslide body is 15.5×10^2 m^2 and the volume is around 27.9×10^3 m^3. The unstable zone is an elongated catchment from which the surface runoff is converged and carried away by a single drainage system draining into the Iazoughen river.

Fig. 6 Landslide inventory map of the study area showing landslides distribution based on the field surveys carried out immediately after the rainfall event of February 2010 and old landslide identified from photo-interpretation and field surveys
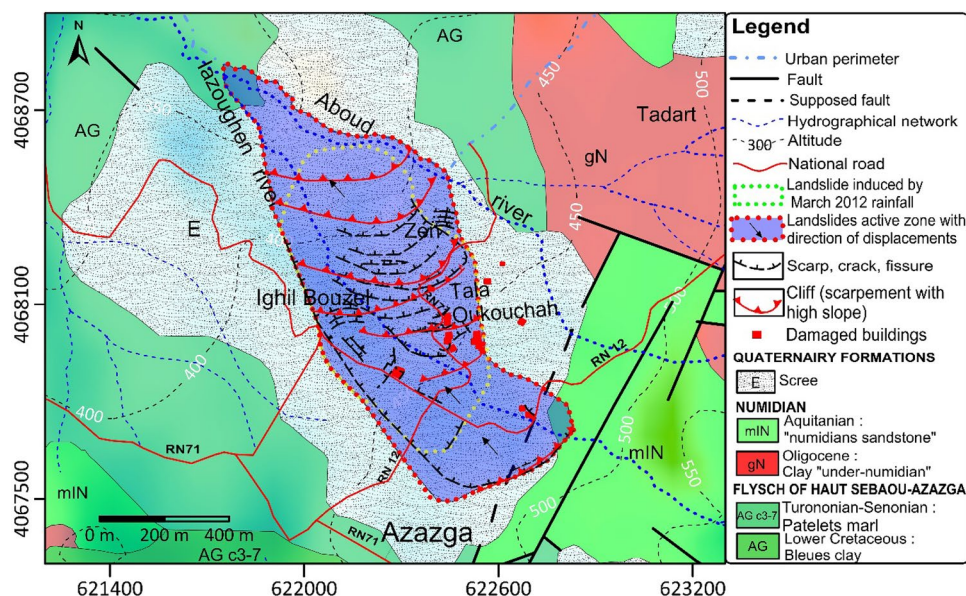
Characteristics and deformation process of the landslide induced by the March 12, 2012 rainfall event

Characteristics of landslide event

After the March 12, 2012 rainfall event, the landform topography had changed significantly after the slope failure that induced a large number of deformations with collapse of national roads, residential buildings developed principally near the head scarp and the body of the landslide. Figure 7 shows the results of field surveys carried out immediately after the rainfall event of March 2012. The rainfall-induced landslide of Ighil Bouzel corresponds to a large complex landslide. The slope movement combines, upstream, translational landslide characteristics (with two juxtaposed plane scarps) and rotational landslide characteristics downstream in the body of the landslide (with several juxtaposed semi-circular scarps). The slope has been sliding towards the Iazoughen River, with active peaks of accelerated movement.

Deformation characteristics based on the field observations

The landslide presents a chaotic topography and a significant series of scarps, subsidence, transverse cracks and bulges parallel to the general slope and separated by cliffs. The landslide has experienced a long deformation history that was observed every year, particularly during the rainy season, showing a potentially high active area with the main scarp. Upstream, the slope is around 10°, while downstream the slope becomes steeper and remains marked by traces of recent activity such as distension and compression cracks, as well as lateral and transverse compression ridges. Figure 7a–f shows the deformation characteristics of the landslide in detail and the locations

Fig. 7 Landslides deformation characteristics observed following heavy rainfall of 2012 in the vicinity of Ighil Bouzel (north of the city of Azazga): **a–c** scarps with an arched shape located at the medium section of the landslide body in the districts of Tala Oukouchah and Zen. **d** Scarps along the national road RN72 in the district of Ighil Bouzel, **e** tensile cracks located within the moving masses in the district of Ighil Bouzel and **f** collapse and stagnation of rainwater at the toe of the landslide. The locations of the photos taken (**a–h**) are shown in Fig. 9

of the photographs are marked in Fig. 9. Many parallel to subparallel tension cracks and fissures are developed as a characteristic of the traction deformation of blocks under high stresses. In the landslide body of the arcuate main scarp (Fig. 7a, b), minor scarps, fissures, depressions, minor landslides, continuous shear surface ground cracks and soil collapses have been observed. The landslide deformation intensified in the middle and the toe parts of the landslide with large cracks, reaching a maximum length of ~ 50 m and a width of ~ 50 cm. The cracks are also observed along the main national roads of RN 12 and RN 71. Tension cracks exhibit lengths ranging from 1 to 50 m, widths of 5 to 30 cm and vertical displacements of 10–60 cm (Fig. 7c, d). Field indices of instability with the inclination of olive trees, leaning of lamp posts, and walls are well observed. Along the flank of the medium section, continuous shear surfaces with lateral levees were observed as well as a centimeter to several meters long fissures and ground settlement (Fig. 7e, f) along the Aboud and Iazoughen waterways. The landslide

toe, sometimes tongue-shaped in plan, is often delineated by a gentle bulge in the ground surface and compression features (Fig. 7f).

Field evidences of previous landslides

Many field observations in and around the landslide zone revealed the existence of previous evidence of instabilities and indicate that the landslides induced by the March 2012 rainfall event constitute partial reactivations of pre-existing landslides. These land instabilities, known since February 1973, were reactivated, respectively, in April 1974, in March 1985, and in March 2012, always following an extended period of rainfall that characterized the winter season. Indeed, field observations showed a high morphological deformation characteristic of low stability slopes with counter slopes, double crests, counterscarps, old scarps and long cliff-like scarps parallel to the general slope trend that are evidence of ancient movements, as can be shown in Fig. 8a–f. This specific morphology is confirmation of

Fig. 8 Examples of ancient land instabilities indicating a mottled morphology with a series of bulges and long cliff-like scarps parallel to the general slope, counter slopes, old scars, characteristic of low stability slopes in the study area. The white dotted points are extend of long cliff, scarps, counter slopes and old scarps. The locations of the photographs (**a–f**) are shown in Fig. 9

Fig. 9 Digital elevation model showing a mottled morphology of slopes stability distribution of landslides during the March 21ᵗʰ, 2012 rainfall event in the study area. Letters (A–H) and (a–h) indicate the localization of photographs of Figs. 7 and 8. Black points correspond to urban perimeter limits, black dotted points are extended of old landslides perimeter, blue dotted points are landslide perimeter induced by the March 2012 rainfall, black lines are scarps observed after March rainfall event, red lines are the long cliff-like scarps
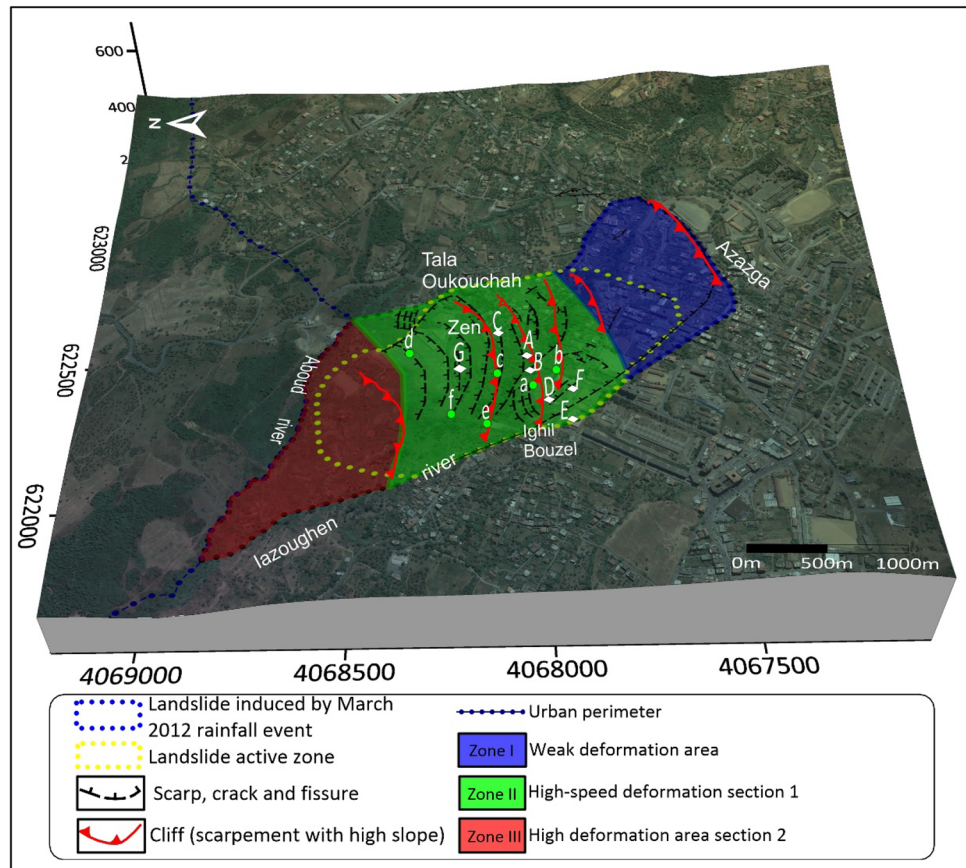
deep-seated landslide deformation that affects hundreds of meters along the Iazoughen River. The cutting zone is reshaped by a series of complex rotational and translational slides. The bodies of landslides are dotted with numerous indicators of "fresh" instability. The downstream area is marked by human activities such as earthworks and backfill surcharges (Fig. 8d, f). The above-cited morphologies are common forms of instabilities that have already functioned in past movements and are still slowly evolving nowadays.

Subzone characteristics

Based on the geomorphological characteristics, deformation characteristics and material structure, the activated landslide area can be divided into three zones (Fig. 9):

- Zone I (weak deformation area): This area is an urban area with a high density of constructions located in the southern part of the investigated region, which is approximately 370 m long and 450 m wide, covering a surface of 1665×10^2 m². Zone I is distinguished by a low deformation upstream showing small deformation features such as cracks and fissures induced by the 2012 rainfall event. The elevation of the upstream area ranges between 440 and 500 m and the mean gradient is 10°.

According to the performed field investigations and borehole data, the geological structure is represented by a thin Quaternary-scree made of clayey to sandy-clay deposits underlying bedrock of the Cretaceous flysch.

- Zone II (high-speed deformation area): Zone II is the accumulation's central sector and it consists primarily of the largest and thickest covered quaternary rock deposits, with a total length of approximately 520 m, a width of 540 m and an area of 2,808,102 m². It involves the largest surface of the 2012 landslide, with expanded, large, heavy and high-speed deformations. The elevation of the downstream zone ranges between 320 and 420 m, with a slope of 5°–10°. The borehole sections revealed that the zone is represented by overlying thick Quaternary-scree deposits (3–31 m) and the underlying bedrock of the Cretaceous flysch.

- Zone III (high deformation area): This area originated in the north-western part of the accumulation, with an irregular shape. It covers an area of about 2760×10^2 m² for approximately 690 m long and 400 m wide. The elevation of the upstream zone ranges between 320 and 420 m for a high slope (> 10°). This area is characterized by a high density of vegetation with high human activity involving modifications of natural morphology by backfill loading, deforestation, and excavation, which increase

the frequency of landslides. Zone III presents high and large deformations with low speed, caused essentially by backfill loading and rainfall.

The landslide-inducing factors

The occurrence of the large Ighil Bouzel landslide can be attributed to two causative factors: (1) the triggering factors related to the antecedent rainfall and human activity; and (2) the susceptibility factors concerning the geology, morphology, hydrogeology and geotechnical characteristics of the soil.

Influence of rainfall on landslides: antecedent rainfall

The historical landslide inventory carried out over the period of 1950–2014 shows that the activation and reactivation of landslides in the city of Azazga are related to the intense rainfall events during the winter season (Fig. 10): 1952 (1190.8 mm), 1955 (992 mm), 1973 (1287.8 mm), 1974 (884 mm), 1984 (1236.1 mm), 1985 (930.7 mm), 2003 (999.6 mm), 2004 (917.6 mm) and 2012 (2086.7 mm). Such a high intensity and accumulation of rainfall can be enough to trigger certain types of landslides, whereas for other types of landslides, an exceptional climatic event is needed. However, the cumulative rainfall has influenced the degree of saturation of the soil and, consequently, plays an important role in the initiation of landslides. Figure 10 shows the cumulative rainfall from December and March for the landslide events over the period of 1950–2014 recorded in the city of Azazga. The peaks of cumulated precipitation over these months reached from the minimal 544 mm in 2003 (54% of the annual amount) to the maximal 886 mm in

2004 (97% of the annual amount) and an average of 691 mm in 2012 (33% of the annual amount). During the winter season of 2012 (December–February), the Azazga region experienced prolonged and intense rainfall with accumulative rainfall exceeding 550 mm, accounting for 55% of the total annual rainfall. From January to March, repeated high-intensity rainfall episodes result in a cumulative peak rainfall of 700 mm, accounting for 65 percent of the annual precipitation (Fig. 10). The first rainfall episode, from January 12th to 17th, was characterized by cumulative precipitation in excess of 80 mm. The second rainfall episode, from 19 to 28th January, was severe, and was as much as 153 mm. The third rainfall episode, from February 2nd to 13th, was characterized by more severe precipitation in the range of 161 mm. The fourth episode, from 18 to 28th February, was characterized by cumulative precipitation of around 71 mm. The last rainfall episode, from 1st to 14th March, was characterized by a cumulative value exceeding 85 mm and a maximum daily rainfall exceeding 20 mm.

During the frequent and cumulative heavy rainfall, the infiltrated water increased the groundwater table level and pore pressure on both the upper-soil slope and the lower-rock slope. This contributed to the alteration of the interlayer material and the degradation of soil mechanical resistance with the loss of shear strength, which finally affected the slope stability.

Local geomorphology

The Ighil Bouzel landslide is initiated on a steep slope that dipped 10°–15° northward (Fig. 11). The slope of the lower rock, with a structure of flysch bedding planes, was relatively steeper than the upper earth's slope, consisting of a thick layer of scree. Field observations showed a mottled morphology and greater deformation with counter slopes, small-displacement sheets, old tearing scars, and small to high scarps that characterize low unstable slopes (Fig. 11). The geomorphological deformation features are more evident on the lower slopes as compared to the upper ones. The morphology of the slope prior to the March 2010 landslide showed an old landslide lobe situated approximately 100 m below the extremity of the March 2012 landslide, suggesting the existence of several long‑runout historical landslides before the contemporary event.

Local geology and structure

The analysis of a lithological section from boreholes in the mainly affected areas, extending from the city to the Iazoughen river, allows us to identify two lithological units (Fig. 12): (1) The Cretaceous flysch bedrock, which is composed of a thick series of gray to greenish clays that are finely bedded, folded, highly fractured and friable, can be
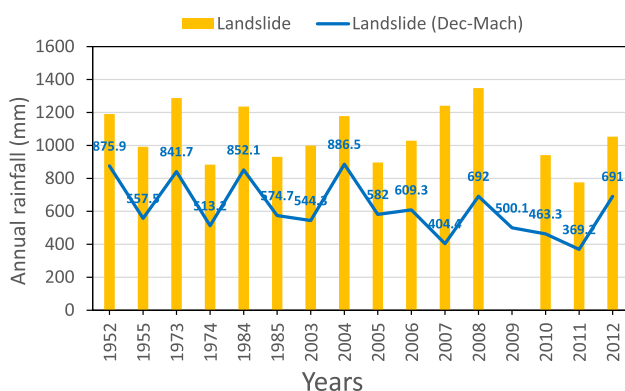
Fig. 10 Relationship between annually rainfalls and cumulative rainfall from December and March for each landslides event for the period of 1950–2014 (meteorological station of Azazga Ecole from ANRH 2019)

Fig. 11 Local geomorphology on digital elevation model with slope gradient classes. Black points correspond to urban perimeter limits, black dotted points are extend of old landslides perimeter, blue dotted points are landslides perimeter induced by the March 2012 rainfall, black lines are scarps observed after March rainfall event, red lines are the long cliff-like scarps
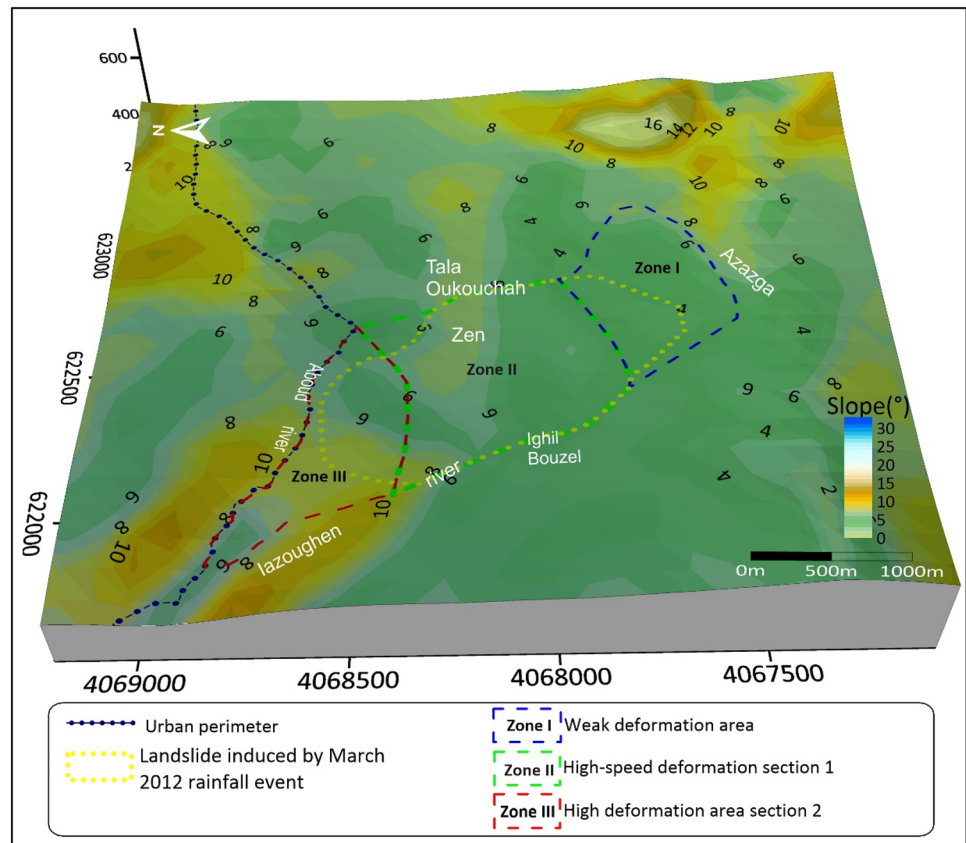
cut into thin platelets at the surface and compact at depth. The depth of the flysch deposit varies between 3 and 31 m as shown in the cross sections AA′ and BB′ of Fig. 12. The depth decreases from the north to the south from 5 to 31 m and from the west to the east from 10 to 25 m; (2) The quaternary screes that cover the Cretaceous flysch are made of sandstone blocks of different sizes embedded in clayey to sandy–clay deposits. Furthermore, the bedding structure of the lower rock slope, with a thin layer of clay beneath the sandstone, has a direct effect on the rock slope's instability due to the ease with which shear-sliding surfaces appear along weak interlayer interfaces. In addition, the lithological discontinuity between the permeable formations (scree) and the impermeable formations (flysch) constitutes a major hydrological discontinuity plane.

Local hydrology and hydrogeology

The study area is crossed by a drainage network essentially represented by the Iazoughen and Aboud permanent flow waterways that have an irregular flow regime, sometimes becoming excessive during the wet season. The "fluvial and torrential" system of the Iazoughen and Aboud rivers passing through the slope toe generates significant runoff saturation of the soil, basal erosion on the banks, and strong undercutting of the slope accompanied by lateral

undermining of the banks, which activates the dynamics of the slope and causes the removal of the abutment of the slope toe, as observed along the Iazoughen river during the heavy rainfall of March 2012 (Fig. 13).

The Quaternary scree deposits overlapping the clay flysch are relatively permeable and allow water to flow through channels, supplying the groundwater table. The relative impermeable clay bedding surface where water accumulates within vertical tension cracks during wet seasons can cause decompression of the marls and the collapse of scree along the versants.

The analysis of the piezometric level map of the mean groundwater table for the high-water period (December–February) based on the inventory of 78 water points (13 piezometers, 4 sources and 60 wells) by using Kriging interpolation shows the presence of a continuous and generalized shallow groundwater with a piezometric level of the groundwater table at a depth ranging between 320 and 450 m and a static level ranging between 2.5 and 5 m (Fig. 14). This groundwater is contained in the quaternary sandy-silty cover formations (scree). The values of the static and piezometric levels of the groundwater table increase from the south to the north, indicating a water flow from the south toward the north and from the center toward the Iazoughen and Aboud rivers in the direction of the landslide (Fig. 12). Figure 12 illustrates the
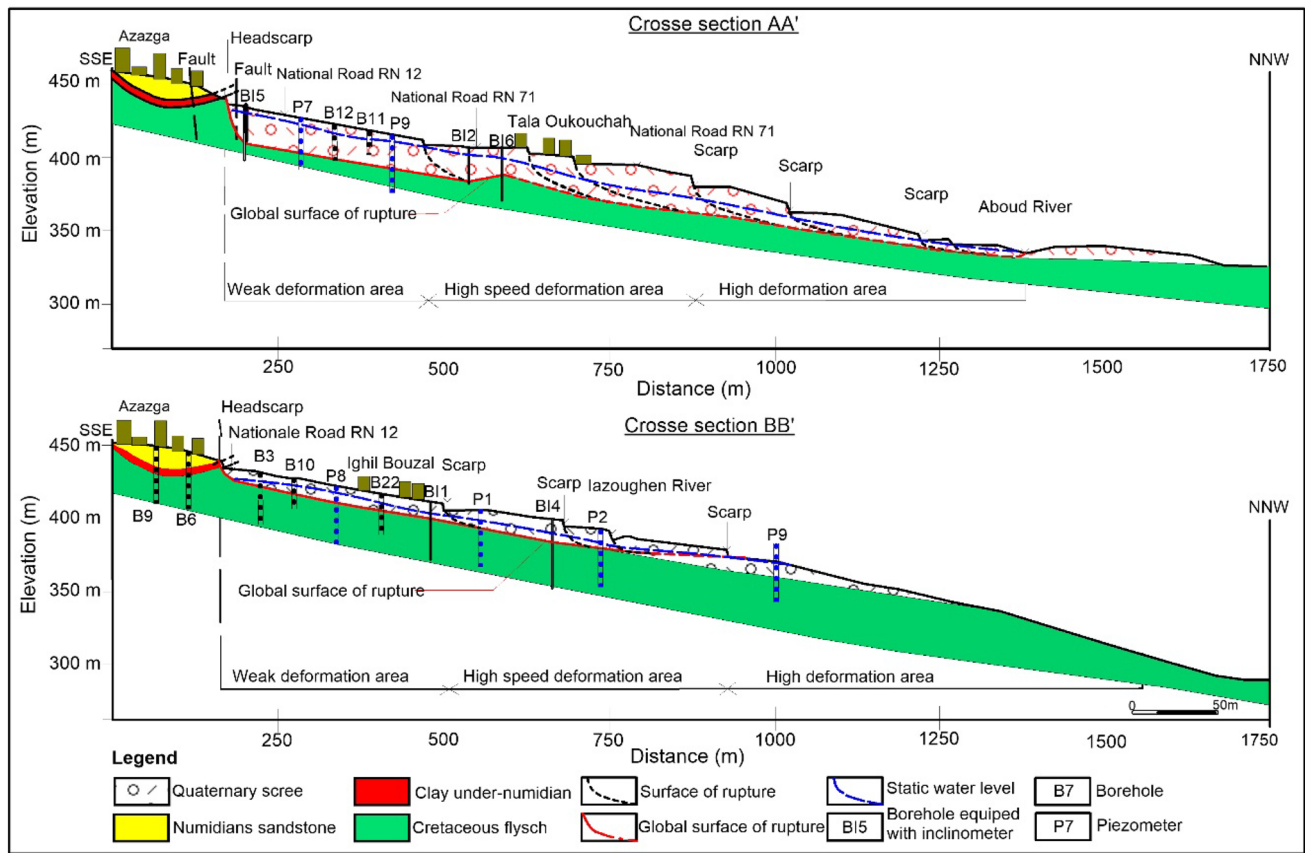
Fig. 12 Geological and hydrogeological cross-sections along the longitudinal profiles AA' and BB' (see Fig. 4 for the locations of the cross sections) in north–south direction performed from borehole, piezometer and inclinometer illustrating the lithological structure with static water level and probable slide surfaces

Fig. 13 Basal erosion and undercutting of the **a** Iazoughen and **b** Aboud rivers torrents at the foot of the landslide area
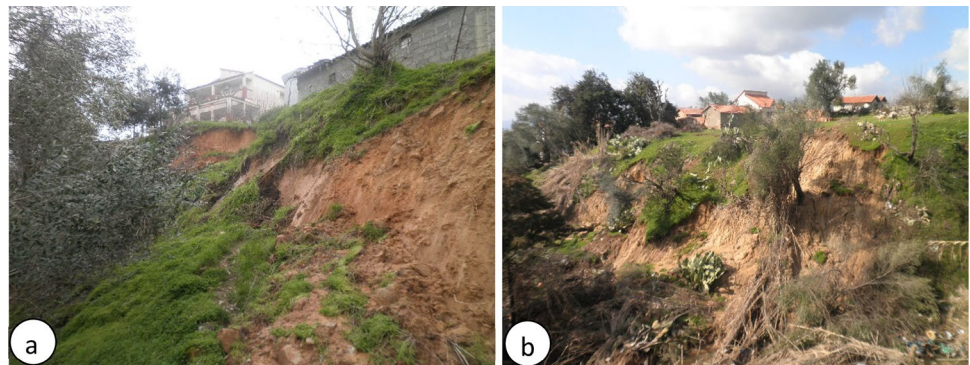
lithological structure of the landslide and the groundwater table in the landslide zone.

Since rainfall is frequently the primary source of the groundwater level in the investigated slope, it is important to understand its response to rainfall. The three piezometers BP1, BP2, and BP3 installed at the bottom of the boreholes (LCTP 2014) along the sliding plane (Fig. 4), indicate a low fluctuation of groundwater level at a depth ranging between 1 and 2.5 m for the period from April 15 to June 15, 2012 (period of groundwater recharge). Low values of groundwater level are observed at the BP2 and BP3 piezometers (0.5–1 m) installed near the toe and body of the landslide, respectively, followed by BP3 values (1–3.4 m) installed at the head of the landslide. Our realistic results indicate that the low value of groundwater level corresponds to the period of groundwater recharge (April to June), then the value increases from June, which corresponds to the discharge period (Fig. 15). There is

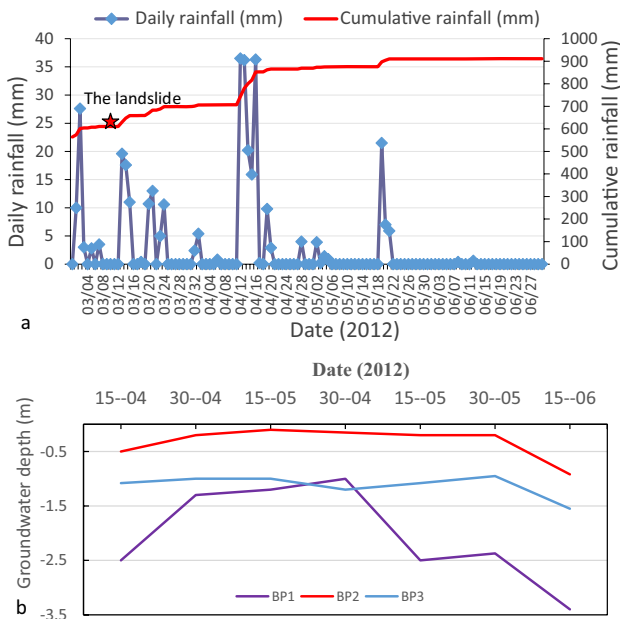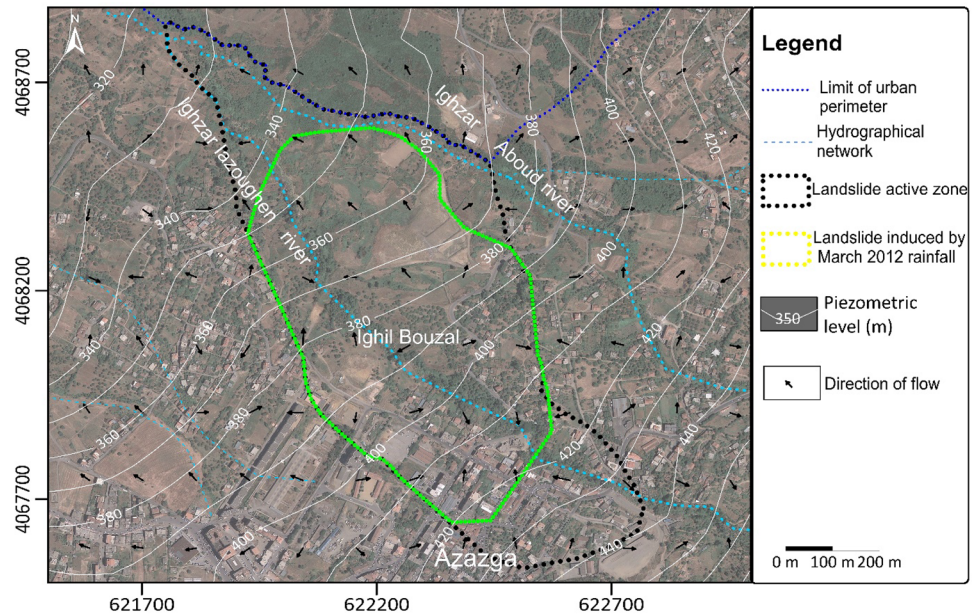**Fig. 14** Static level (SL) map of the groundwater table in study area

Fig. 15 Relationship between: **a** normal cumulative potential precipitation and **b** groundwater level fluctuations monitored by piezometers installed along the sliding plane for the period from April 4, 2012 to December 25, 2013

a good relationship between normal cumulative precipitation (Fig. 15a) and groundwater level (Fig. 15b). The shallow depth of groundwater level is related to the saturation conditions caused by continual cumulative precipitation increasing the water content of the sliding mass, as observed during heavy rainfall events through sources, springs and wells (Fig. 16a, b) in the upstream part of the

landslide and in the landslide toe (Fig. 16c, d), leading to a major loss in the shear strength of the sliding zone.

Geotechnical characteristics

The statistical analysis of the geotechnical data allowed us to distinguish three geotechnical units (Table 1): (1) the weathered greenish-grey clay unit corresponds to the upper part of the flysch substratum. This unit coincides with fine soil (56 < Fc < 98%) that is moderately dense ($1.35 < \gamma_d < 1.88$ t/m^3), saturated (Sr of 93%), plastic and very sensitive to the presence of water (LL varies between 48 and 77 and PL between 20 and 37). The oedometric tests showed a fairly to moderately compressible soil (Cc between 11 and 24) and swellable soil (Cs between 2.8 and 9); (2) the compact grey-blue clay unit corresponds to the compact part of the Cretaceous flysch substratum at depth. The statistical analysis of the physical parameters, showed a fine soil (55 < Fc < 100%), of average density that increases strongly with depth (γ_d ranges between 1.52 and 2 t/m^3). The degree of saturation reaches 100% in the first few meters and then Sr = 37% at depth. The soil is classified as not very plastic (LL = 50 and PL = 22). Shear tests showed deep and undisturbed clay. The oedometric tests classify the soil as moderately compressible (Cc around 20) and swellable (Cs around 8); (3) The sandy-clay scree unit corresponds to multi-sized sandstone blocks, embedded in sandy-clay deposits. The granulometric analysis, shows sands and clays presenting 15–97%, respectively, of grain size. The physical characteristics revealed a nonsaturated to saturated soil (10 < Sr < 90%), low to high density ($1.4 < \gamma_d < 1.93$ t/m^3) and low to medium plasticity (LL = 23 to 35 and PL = 7 to 35). The results of the oedometer tests reveal sandy clays that are moderately compressible (Cc ranging between 6 and 34)

Fig. 16 Observed groundwater table in the study area: **a**, **b** wells and water spring showing the surface water level during wet periods in the upstream part of the landslide, **c**, **d** Groundwater discharge at the landslide toe after the 12, March 2012 rainfall event

and not very swellable (Cs ranging between 2 and 11). The geotechnical tests results showed that the upper part of the flysch bedrock is plastic, weathered and very sensitive to water infiltration with low mechanical strength and easy formation of a shear slipping surface (geotechnical interface) along this weak interlayer and, consequently, ultimately susceptible to landslide. The sliding zone is a continuous, thick shear zone located in the weathered upper part of the flysch.

The human activity

The human activity represented by intense and fast-unplanned urbanization, mainly since 1978, has led to significant morphological changes in the stability conditions through deforestation, excavation, embankments, slope cutting for constructions, and road openings, thus increasing the frequency of the Ighil Bouzel landslide. The main engineering activities are represented by various excavations for buildings, national roads (RN 12 and 71), and municipality ways at the head of the slope and the embankments at the slope toe (Figs. 16c, d, 7f). This loading of the embankments and excavations degraded the quality of the rock mass and moved the lower rock slope towards a disequilibrium unstable state, which finally contributed to the slope failure initiation.

Mechanism analysis

The characterization of the dynamic nature of the unstable slope, particularly the identification of the shape and depth of the failure surfaces, was possible based on the information gathered from field observation, analysis of the inclinometers measurements results and ERT investigations. The field observations showed several indications of instability, such as an irregular morphology resulting from the existence of several different ground failure lines and scarps.

Inclinometers data interpretation

As shown in Fig. 4, six inclinometer tubes were installed in six boreholes (BI1, BI2, BI3, BI4, BI5 and BI6) along the Ighil Bouzel landslide at a depth varying from 24 to 36 m. The measurements and the monitoring were performed from April 16, 2012, to December 25, 2013. The results of inclinometers measurements are correlated with the boreholes. Table 2 summarizes the results of these measurements. The depths of the flysch rocks from BI1 to BI6 are 12, 25, 24, 19, 28 and 10 m, respectively.

The results of Fig. 17 show that (Table 2): (1) the depth of the failure surface varies from a minimum of 11 m to maximum of 29 m; (2) the cumulative displacements at the crown of the inclinometers are from 0.06 to 3.45 cm; (3) the cumulative displacement and displacement rate at the top of BI5 are larger as compared to the other four inclinometers; (4) the cumulative displacement and rate of the major sliding plane at BI1, BI2, BI3 and BI4 are larger than BI5 and BI6 inclinometers; (5) The BI1, BI2, BI3 and BI4 inclinometers show higher evolution speeds than BI5 and BI6; (6) the mass slide is moving in the northwest direction toward the Iazoughen and Aboud rivers; and (7) the mean displacement for the period 2012–2013 is approximately 0.003 cm to 0.076 cm day^{-1} i.e. a magnitude of 1 cm to 28 cm year^{-1}.

Table 2 Results of inclinometer measurements for the period from 16 April 2012 to 25 December 2013

Inclinometer	Elevation	Depth of borehole (m)	Depth of sliding surfaces (m)	Cumulative displacement at top of inclinometer tubes (cm)	Mean displacement rate at top of inclinometer tubes (cm)	Displacement rates of sliding plane (cm/days)	Mean displacement of sliding plane (cm/days)
BI 1	395.490	32.50	11.5	0.14	0.64	0.04–0.06	0.050
BI 2	392.942	35.00	24.5	0.03	0.43	0.01–0.04	0.025
BI 3	398.400	34.50	27	0.08	2.15	0.06–0.09	0.076
BI 4	381.177	35.00	14–18	0.01	0.55	0.02–0.03	0.023
BI 5	441.679	36.00	28–29	0.02	0.06	0.03–0.05	0.003
BI 6	414.058	35.00	14	0.05	3.45	0.005–0.01	0.010

These inclinometer results suggest a deep deformation, with the failure surface located along the interface between the flysch bedrock and the overlying scree. In addition, the surface of the rupture is located below the water table level. According to the hydrogeological structure (Fig. 12), the possibility of several superimposed failure surfaces cannot be excluded. The sliding zone corresponds to the weathered upper part of the flysch bedrock (shear zone). The geotechnical characteristics of the soil in the sliding zone (geotechnical interface) confirm a saturated, plastic soil with low cohesion and low angles of friction (Table 1). The shear zone is moderately compressible, swellable, and consequently very sensitive to the variation of water content.

The landslide is influenced and governed mostly by the basal regressive erosion and undercutting of the Iazoughen and Aboud river torrents that degenerate the toe of the slope. This is justified by the higher evolution speeds given by the BI1, BI2, BI3 and BI4 inclinometers located close to the Iazoughen river. According to the classification of Lateltin (1997), the actual mean velocity makes the Ighil Bouzel an active to very active landslide with fast phases.

The electrical resistivity tomography (ERT) data interpretations

The ERT test is considered the most adequate and efficient geophysical method for the identification of the depth and internal structure of slope deformations (such as main body, physical properties, water content, geometry and position of the shear surface) based on the spatial distribution of electrical resistivity contrasts of the soil provided by 2D or 3D images (Hack 2000; Havenith et al. 2000; Mahmut et al. 2006; Jongmans and Garambois 2007; Perrone et al. 2014; Omowumi Falae et al. 2019).

In this study, the ERT survey was conducted on the first week of January 2020 in a landslide area by CGS along four profiles of dipole array device configuration using 48 electrodes cable 2.5 m apart with rolling. The profiles 1 and 4 were performed along the axis of the landslide, while the profiles 2 and 3 were conducted across the landslide body (Fig. 18). The data was processed by a resistivity inversion technique using RES2DINV software to achieve electrical imaging along these lines. The results presented in Fig. 18 show the lateral and depth variation of the resistivity. The obtained tomograms are combined and calibrated with the boreholes and inclinometers. A good concordance between resistivity and inclinometers results was noted.

The profile 1 was in the direction of NW–SE over a length of about 355 m. The profile crosses the borehole BI 2, equipped with an inclinometer that shows a failure surface at a depth of 24 m. The resulting tomogram along this profile indicates two distinct resistivity zones along the line. The zone of low resistivity (10–20 Ω m), located in all the sections at a depth of 20–50 m, probably represents the landslide materials with higher water content. The zone of high resistivity corresponds to the sandstone screes. The landslide material, clay, sand and sandstone block units observed in the borehole are in good agreement with the results of the electrical resistivity tomography. The resistivity values strongly decrease with depth in the clay of the flysch unit. The presence of water is indicated by low resistivity values, which is the key parameter in slide initiation.

The profile 2 of about 475 m in length in the direction of NE to SW passes through the borehole BI 4 equipped with an inclinometer at a depth of 35 m. The resistivity distribution is low (10–20 Ω m) in the north-eastern part and in the middle of the profile (between 0 and 10 m), while it is rather high (20 and 300 Ω m) in the south-western part of the profile (between 0 and 40 m). At depth, resistivity values are very low (< 10 Ω m) in the north-eastern and middle parts of the profile (between 35 and 60 m). The low resistivity might be caused by the water content of the unconsolidated material (scree sandstone), while the higher values might be an indicator of the consolidated materials (sandstone blocks). The results show the resistivity contrast that corresponds to the geological interface between the quaternary scree deposits and the Cretaceous flysch substratum. Thus, the presence of an interface, identified by the borehole data, is clearly verified by the resistivity results.

Fig. 17 Cumulative horizontal displacement versus the depth of inclinometers for the period from 16.04.2012 to 25.12.2013. The inclinometer readings are compared and superimposing to the boreholes section
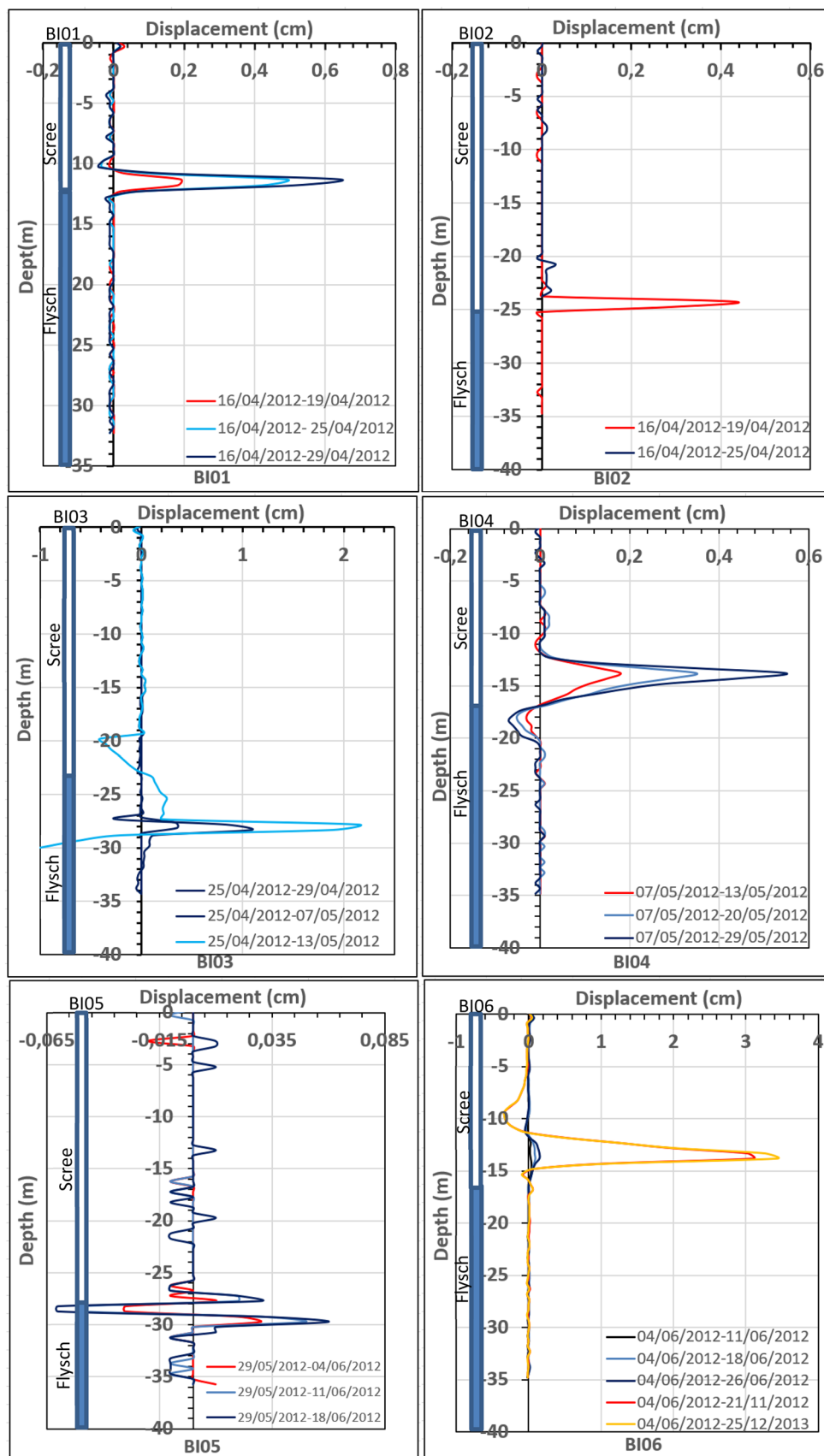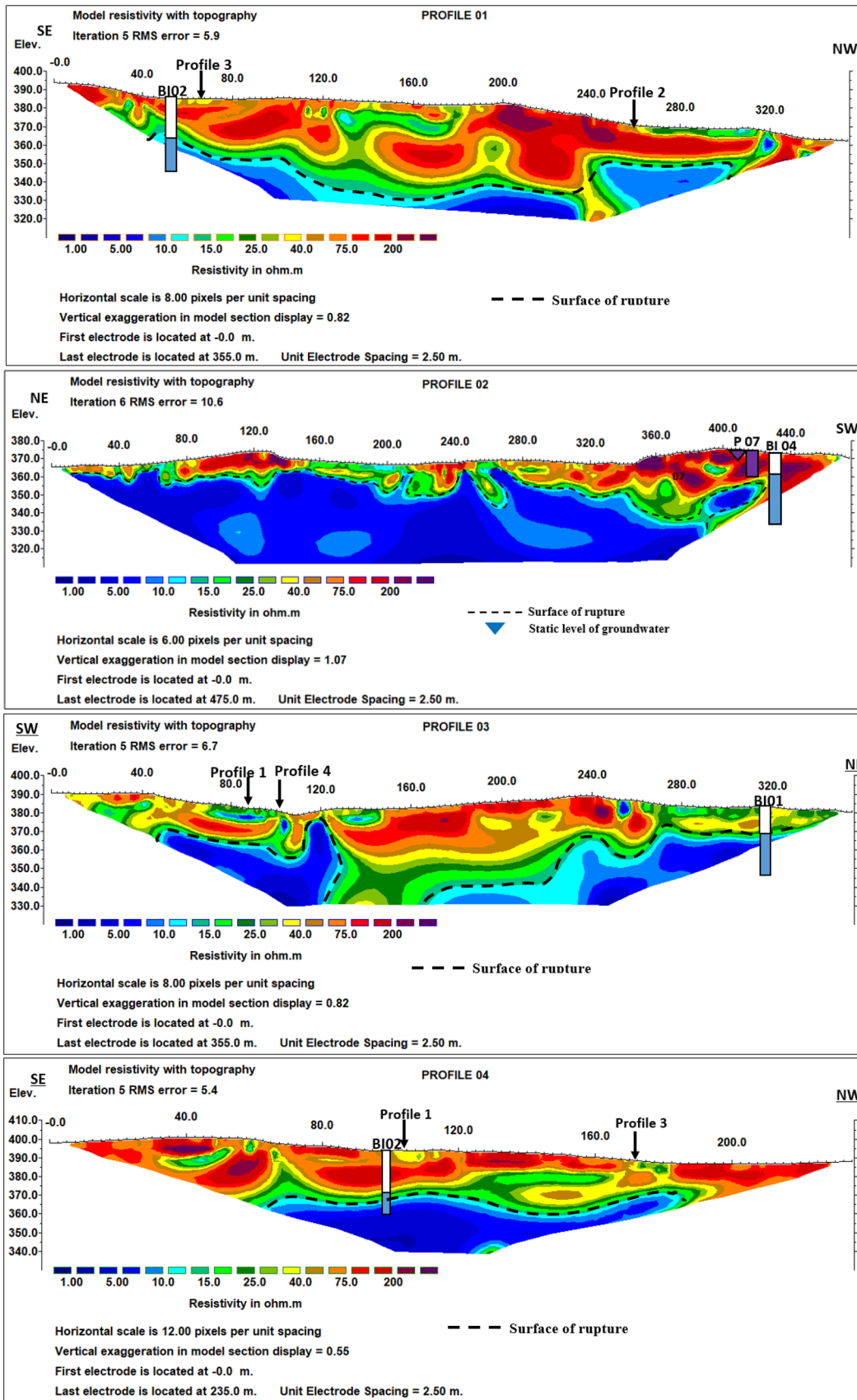
◄**Fig. 18** Electrical resistivity tomography results: profile 1 and profile 4 obtained along the direction of landslide movement, profile 2 and profile 3 performed along the perpendicular direction to the landslide movement (profile location is shown in Fig. 4). The black arrow corresponds to the location and intersection of the different profiles

The third profile crosses the direction of the landslide movement over about 355 m in length. The profile 3 was performed in the direction of NE–SW and passed through the borehole BI1 equipped with an inclinometer at a depth of 32 m. The obtained ERT result revealed the rupture surface and the subsurface geometry of the landslide. It is considered that the relatively high resistivity layer (15–250 Ω m) observed at shallow depths might be derived from the landslide material. The thickness of this layer varies between 5 and 15 m on the tomogram. Furthermore, the electrical tomography image is in good agreement with the results of the borehole, showing the depth of the landslide that was confirmed by the borehole data.

The profile 4 was in the continuity of the profile 1 in the direction of the landslide over a length of about 235 m. The profile passes through the borehole BI 2, equipped with an inclinometer at a depth of 35 m. The ERT result shows that the scree layer (clay, sand and sandstone) with relatively high resistivity (15–250 Ω m) blocks is observed at depths ranging between 20–40 m, which might be originated by the landslide material composed of unconsolidated and water-saturated landslide material. The zone of relatively very low resistivity (05–10 Ω m) between the depths of 20–40 m corresponds to the clays of the flysch unit formed by the consolidated deposits. Thus, the roof of this layer may correspond to the failure surface of the recent landslide. The resistivity results were confirmed by the borehole data of BI 2 that showed a surface of rupture at a depth of 24 m.

The intersection of the obtained results from the four profiles shows clearly the identical depth and internal structure of the landslide based on the spatial distribution of electrical resistivity contrasts in the soil. Crossing profile 1 with profiles 2, 3 and 4 indicates equal depth of a failure surface of 25 m. The connection of profile 3 with profile 4 gives a similar depth of a sliding surface of around 20 m.

The ERT method applied in our landslide area study case has allowed us to characterize the geometry (shape of the slope, body and surface of rupture) of landslides. The electrical resistivity values along the performed profiles reveal a structure composed of a layer of displaced scree materials with relatively high resistivity, superimposed on the clayey substratum, which has low resistivity. The resistivity results were confirmed by the results of boreholes equipped with inclinometers.

According to the deformation process and mechanism modes, the Ighil Bouzel landslide corresponds to a complex deformation mechanism with a complex and progressive failure along the geotechnical interface located in the upper part of the flysch bedding rock slope. The landslide is favored and controlled essentially by: (1) the lithological discontinuity or interface in the contact zone scree/flysch; (2) the dip of the flysch conforming to the slope; (3) the dip of the schistosity and the diaclase planes of the flysch in the slope direction; and (4) the basal erosion and undercutting of the Iazoughen and Aboud river torrents.

Discussion and conclusion

The complexity of large, deep-seated landslides is represented by the difficulty of determining their critical prior-failure conditions and forecasting future behavior, which constitute a serious issue for scientists. Multiparameter monitoring, physically based models and landslide inventory mapping using remote sensing technology are promising approaches that have recently been applied in several studies (Guzzetti et al. 2004, 2012; Chen et al. 2006; Booth et al. 2009; Mondini et al. 2011; Martha et al. 2012; Prokešová et al. 2014; Laribiet al. 2014; Bhambri et al. 2016; Borgomeo et al. 2014; Laribi et al. 2014; Crosta et al. 2014; Jaboyedoff et al. 2016; Su et al. 2017; Hallal et al. 2017).

In this research, we use a highly recommended approach for large scale areas based on the landslide inventory mapping combined with extensive field investigation to analyze the deformation characteristics, the controlling factors and the failure mechanisms of the large landslide induced by a rainfall event in the city of Azazga (Northern Algeria).

Landslide inventory mapping revealed that the March 2012 landslide, which affected a total surface of 0.40 km², was a partial reactivation of large pre-existing landslides covering an area of 570.400 m², approximately 6.26% of the total urban area. The initiation and reactivation of this large rainfall-induced landslide resulted from a combination of the triggering factors as well as susceptibility factors.

Seasonal intense rainfall is certainly the main triggering factor of landslides in the study region. Such high intensity and the cumulative or antecedent rainfall play an important role in the initiation or reactivation of landslides. The monitoring deformation with inclinometers in 2012 and 2013 indicated a deep cumulative displacement of less than 0.09 cm and a surface cumulative displacement of less than 0.14 cm, for an average of 0.055 cm. The monthly rainfalls (January to March) during the activation of the landslide (2012) were all greater than the average annual values. It seems that the slope mass movement was closely related to the amount of rainfall. Earlier reported analyses showed the critical role of cumulative rainfall episodes with high intensity over an interval of days. From January to March, repeated rainfall episodes were characterized by high-intensity cumulative precipitation (Fig. 5). The cumulative peak

rainfall reached 19.6 mm during a period of 24 h, exceeding 85 mm from March 1st to March 12th and exceeding 550 mm from January to March 2012. The variation of groundwater depth, monitored from April 2012 to December 2013, indicates a good relationship between normal cumulative precipitation and groundwater level. The low depth of groundwater level is related to the cumulative precipitation that has highly influenced landslide reactivation.

Groundwater level measurements from piezometers installed along the sliding plane for a short period indicate that cumulative precipitation and consequent groundwater level increase play an important role in deep-seated failure initiation in specific geological conditions. In addition, the amount of displacement or even the reactivation was always correlated with the amount of precipitation. With the limited available data, it was still difficult to quantify the relationship between the amount of displacement and the amount of rainfall. However, the velocity of surface displacement is more closely related to the groundwater level and the groundwater table depth of between 2.5 and 5 m can serve as a warning threshold in this specific case. Positive pore pressure on the potential slip surface induced by rising groundwater levels is considered to be the main mechanism leading to failure in hydrologically triggered deep-seated landslides. Therefore, it is believed that deeper landslides are reactivated when abnormally high precipitation continues over a long period, often lasting for several months to several years (Corominas and Moya 1999; Gil and Długosz 2006; Burda and Vilímek 2010; Gattinoni et al. 2012). Conversely, some authors have pointed out that the characteristics of long-term movements in deep-seated landslides are more closely related to the hydrological factor of water content in the slope than to the pore-water pressure increase on the potential slip plane (Matsuura et al. 2008; Prokešová et al. 2014). Consequently, land movements may be the result of other mechanisms by which the groundwater level acts to support slope failure. Thus, the water content can be directly correlated to rainfall or effective rainfall and should be considered as a very important factor controlling deep-seated landslide behavior (Crozier 1999; Matsuura et al. 2008; Prokešová et al. 2014).

Considering the importance of groundwater level in slope stability, we should take measures to reduce groundwater's effect in order to improve landslide stability, such as drainage through deep trenches or galleries combined with radial draining drilling, digging and an annular intercepting drain above the trough at the back edge of the landslide, which could prevent the surface from gathering and flowing into the landslide.

Four susceptibility factors, geological structure, hydrogeological condition, geotechnical characteristics, and morphological condition, have adverse effects on the failure of this complex landslide. The flysch bedding structure of the overlying bedrok is folded, highly fractured and friable, with an underlying scree of soft soil (clay and sandstone). The upper-earth slope is comprised of a loose and porous soil layer overlying the impermeable flysch bedrock, which makes it favorable for surface water infiltration and groundwater retention. Moreover, the weak mechanical resistance characteristics of the upper part of the flysch bedrock with a thin layer of clay, very sensitive to water infiltration, have a direct influence on the instability of the rock slope due to the easy formation of a shear slipping surface along the weak interlayers. In addition, morphological conditions of the steep slope and mottled morphology with greater deformations are confirmations of deep-seated and evidence of partial reactivations of pre-existing landslides. However, we conclude that rainfall, coupled with the internal geological conditions such as the separated geomorphic unit, the flysch bedding slope structure of the overlying hard rock and underlying soft rock, the weak interlayers and the previous slope excavations, drove the slope towards a disequilibrium/unstable state and final failure.

According to the inclinometers and ERT results, the landslide is a type of "deep-seated" landslide with failure surfaces at a depth ranging between 11 and 29 m and a "high-speed process" with an average velocity of 1–29 cm year^{-1}. Moreover, considering the geomorphologic characteristics and the shape of the slip surfaces, the landslide exhibited a complex failure mode with a slip surface located along geotechnical interfaces between the flysch bedrock and the overlying quaternary scree. According to the mechanism modes, the slope movements are located in the saturated and weathered zone within the Cretaceous flysch strata favored and controlled essentially by: (1) the lithological discontinuity in the contact zone scree/flysch; (2) the dip and the tectonic structure of the flysch in the slope direction; and (3) the destabilization of the slope by the basal undercutting by the Iazoughen and Aboud rivers' torrents.

In agreement with prior studies conducted in various regions of the world, this research clarifies the competing roles that local factors play in determining the incidence and frequency of landslides and contributes to a better understanding of landslide events in the Azazga agglomeration region (Corominas and Moya 1999; Dai and Lee 2001; Chau et al. 2004; Gil and Długosz 2006; Macfarlane 2009; Burda and Vilímek2010; Goswami et al. 2011; Guzzetti et al. 2012; Gattinoni et al. 2012; Gullàet al. 2012; Prokešová et al. 2014; Borgomeo et al. 2014; Laribi et al. 2014; Crosta et al. 2014; Jaboyedoff et al. 2016; Su et al. 2017; Hallal et al. 2017; Ouyang et al. 2018; Wang et al. 2019; Li et al. 2019; Bourenane et al. 2021a). Our results support the previously published ideas that cumulative rainfall episodes play an important role in evolving instability in rainfall triggering large deep-seated landslides (Iverson and Major 1987; Corominas and Moya 1999; Van Asch

et al. 1999; Rybář 2006; Burda and Vilímek 2010; Gattinoni et al. 2012; Matsuura et al. 2008; Burda and Vilímek 2010; Prokešová et al. 2014). Therefore, the rainy season (although not exceptionally rainy) following a prolonged wet period can be more responsible for movement acceleration and/or failure initiation than an exceptionally rainy season following a dry period of considerable length. The obtained results also indicate that in this part of Algeria, lithology, tectonics, land use and long-term fluvial erosion/undercutting essentially control landslide occurrence; this implies that large landslides may be more common in flysch zones where hill slope gradients are between 10° and 20° and close to watercourses. As a result, this is where mitigation efforts should be focused. Consequently, this comprehensive research provides an exhaustive understanding of the deformation features and failure mechanisms of rainfall-induced large landslides in urban areas as well as useful information for landslide hazard and risk mitigation. The findings can be used to guide future research into assessing and forecasting landslide hazard, vulnerability and risk.

Declarations

Competing interests The author have no competing interests to declare that are relevant to the content of this article.

Ethics approval Not applicable.

Consent to participate Not applicable.

Consent for publication Not applicable.

References

Agence Nationale des Ressources Hydriques ANRH (2019) Precipitation database covering a time-period of 32 years from the 3 meteorological stations: "Azazga Ecole, Yakourene and Freha"

Bhambri R, Mehta M, Dobhal DP, Gupta AK, Pratap B, Kesarwani K, Verma A (2016) Devastation in the Kedarnath (Mandakini) Valley, Garhwal Himalaya, during 16–17 June 2013: a remote sensing and ground-based assessment. Nat Hazards 80:1801–1822. https://doi.org/10.1007/s11069-015-2033-y

Booth AM, Roering JJ, Perron JJ (2009) Automated landslide mapping using spectral analysis and high-resolution topographic data: Puget Sound lowlands, Washington, and Portland Hills, Oregon. Geomorphology 109:132–147. https://doi.org/10.1016/j.geomorph.2009.02.027

Borgomeo E, Hebditch KV, Whittaker AC, Lonergan L (2014) Characterising the spatial distribution, frequency and geomorphic controls on landslide occurrence, Molise, Italy. Geomorphology 226(1):148–161. https://doi.org/10.1016/j.geomorph.2014.08.004

Bourenane H, Bouhadad Y, Guettouche MS, Braham M (2014) GIS-based landslide susceptibility zonation using bivariate statistical and expert approaches in the city of Constantine (Northeast Algeria). Bull Eng Geol Environ. https://doi.org/10.1007/s10064-014-0616-6

Bourenane H, Guettouche MS, Bouhadad Y, Braham M (2016) Landslide hazard mapping in the Constantine city, Northeast Algeria using frequency ratio, weights factor, logistic regression, weights of evidence, and analytical hierarchy process methods. Arab J Geosci. https://doi.org/10.1007/s12517-015-2222-8

Bourenane H, Meziani AA, Ait Benamar D (2021) Application of GIS-based statistical modeling for landslide susceptibility mapping in the city of Azazga, Northern Algeria. Bull Eng Geol Environ. https://doi.org/10.1007/s10064-021-02386-0

Bourenane H, Braham M, Bouhadad Y, Meziani AA (2021) Spatial distribution, controlling factors and failure mechanisms of the large-scale landslides in the urban area of Azazga city (Northern Algeria). Environ Earth Sci 80:313. https://doi.org/10.1007/s12665-021-09607-5

Bowles JE (1992) Engineering properties of soils and their measurements. McGraw-Hill, New Jersey

Burda J, Vilímek V (2010) The influence of climate effects and fluctuations in groundwater level on the stability of anthropogenic foothill slopes in the KrušnéHory Mountains, Czechia. Geografie 115(4):377–392

CGS (2010) Etude de microzonage sismique de la ville de Azazga (Etape A2 : Carte photogéologique). Unpublished Internal report

CGS (2014) Des campagnes piézométriques réalisées pour l'étude de Microzonage sismique de la ville d'Azazga. Unpublished Internal report

CGS (2018) Seismic microzoning study of the city of Azazga. National Center of Applied Research in Earthquake Engineering CGS (Etape A3: Carte géotechnique et données hydrogéologiques). Unpublished Internal report

CGS (2020) Des campagnes géophysiques réalisées pour l'étude de Microzonage sismique de la ville d'Azazga. Unpublished Internal report

Chau KT, Sze YL, Fung MK, Wong WY, Fong EL, Chan LCP (2004) Landslide hazard analysis for Hong Kong using landslide inventory and GIS. Comput Geosci 30(4):429–443. https://doi.org/10.1016/j.cageo.2003.08.013

Chen RF, Chang KJ, Angelier J, Chan YC, Deffontaines B, Lee CT, Lin ML (2006) Topographical changes revealed by high-resolution airborne LiDAR data: the 1999 Tsaoling landslide induced by the Chi-Chi earthquake. Eng Geol 88:160–172. https://doi.org/10.1016/j.enggeo.2006.09.008

Corominas J, Moya J (1999) Reconstructing recent landslide activity in relation to rainfall in the Llobregat River basin, Eastern Pyrenees, Spain. Geomorphology 30:79–93. https://doi.org/10.1016/S0169-555X(99)00046-X

Crosta GB, di Prisco C, Frattini P, Frigerio G, Castellanza R, Agliardi F (2014) Chasing a complete understanding of the triggering mechanisms of a large rapidly evolving rockslide. Landslides 11:747–764. https://doi.org/10.1007/s10346-013-0433-1

Crozier MJ (1999) Prediction of rainfall-triggered landslides: a test of the antecedent water status model. Earth Surf Process Landf 24:825–833

Dai FC, Lee CF (2001) Frequency-volume relation and prediction of rainfall-induced landslides. Eng Geol 59(3–4):253–266. https://doi.org/10.1016/S0013-7952(00)00077-6

Dai FC, Lee CF (2002) Landslide characteristics and slope instability modeling using GIS, Lantau Island, Hong Kong. Geomorphology 42:213–228. https://doi.org/10.1016/S0169-555X(01)00087-3

Djerbal L, Alimrina N, Melbouci B, Bahar R (2014) Mapping and management of landslide risk in the city of Azazga (Algeria). In: Landslide science for a safer geoenvironment. Springer International Publishing, pp 463–468. https://doi.org/10.1007/978-3-319-05050-8_72

Gattinoni P, Scesi L, Arieni L, Canavesi M (2012) The February 2010 large landslide at Maierato, Vibo Valentia, Southern Italy. Landslides. https://doi.org/10.1007/s10346-011-0296-2

Gelard J.P (1979) Géologie du Nord – Est de la Grande Kabylie (un segment des zones interne de l'orogène littoral maghrébin)—Thèse de doctorat

Gil E, Długosz M (2006) Threshold values of rainfalls triggering selected deep-seated landslide in the Polisch Flysch Carpathians. Studia Geomorphologica Carpatho-Balcanica 40:21–43

Goswami R, Mitchell NC, Brocklehurst SH (2011) Distribution and causes of landslides in the eastern Peloritani of NE Sicily and western Aspromonte of SW Calabria, Italy. Geomorphology 132(2011):111–122. https://doi.org/10.1016/j.geomorph.2011.04.036

Gullà G, Caloiero T, Coscarelli R, Petrucci O (2012) Rainfall–landslide scenarios: amethodological application in Calabria (Southern Italy). Nat Hazard Earth Syst Sci 12:165–173

Guzzetti F, Cardinali M, Reichenbach P, Cipolla F, Sebastiani C, Galli M, Salvati P (2004) Landslides triggered by the 23 November 2000 rainfall event in the Imperia Province, Western Liguria, Italy. Eng Geol 73(2):229–245. https://doi.org/10.1016/j.enggeo.2004.01.006

Guzzetti F, Mondini AC, Cardinali M, Fiorucci F, Santangelo M, Chang K (2012) Landslide inventory maps: new tools for an old problem. Earth Sci Rev 112(1–2):42–66. https://doi.org/10.1016/j.earscirev.2012.02.001

Hack R (2000) Geophysics for slope stability. Surv Geophys 21:423–448. https://doi.org/10.1023/A:1006797126800

Hallal N, Dubois L, Bougdal R, Djouder F (2017) Instabilités gravitaires dans la région de Bejaia (Algerie): inventaire et appréciation de l'importance relative des différents paramètres conduisant au déclenchement, au maintien ou à l'activation des instabilités. Bull Eng Geol Environ. https://doi.org/10.1007/s10064-017-1050-3

Harp EL, Keefer DK, Sato HP, Yagi H (2011) Landslide inventories: the essential part of seismic landslide hazard analyses. Eng Geol 122(1–2):9–21. https://doi.org/10.1016/j.enggeo.2010.06.013

Havenith HB, Jongmans D, Abdrakhmatov K, Trefois P, Delvaux D, Torgoev IA (2000) Geophysical investigations of seismically induced surface effects: case study of a landslide in the Suusamyr valley, Kyrgyzstan. Surv Geophys 21:349–369. https://doi.org/10.1023/A:1006788808145

Iverson RM, Major JJ (1987) Rainfall, groundwater flow, and seasonal movement at Minor Creek landslide, northwestern California: physical interpretation of empirical relations. Geol Soc Am Bull 99:579–594

Jaboyedoff M, Oppikofer T, Abellán A, Derron MH, Loye A, Metzger R, Pedrazzini A (2012) Use of LIDAR in landslide investigations: a review. Nat Hazards 61(1):5–28. https://doi.org/10.1007/s11069-010-9634-2

Jongmans D, Garambois S (2007) Geophysical investigation of landslides: a review. Bull Soc Geol Fr 178(2):101–112

Laribi A, Walstra J, Ougrine M, Seridi A, Dechemi N (2014) Use of digital photogrammetry for the study of unstable slopes in urban areas: case study of the El Biar landslide, Algiers. Eng Geol 187(2015):73–83. https://doi.org/10.1016/j.enggeo.2014.12.018

Lateltin O (1997) Prise en compte des dangers dus aux mouvements de terrain dans le cadre des activités de l'aménagement du territoire. Recommandations. Office fédéral de l'aménagement du territoire (OFAT), Office fédéral de l'économie des eaux (OFEE), Office fédéral de l'environnement, des forêts et des paysages (OFEFP)

LCTP (2012) Etude géotechnique du POS A1 et A5. Unpublished Internal reports. Laboratoire des Travaux Publics

LCTP (2014) Etude géotechnique du POS A1 et A5. Unpublished Internal reports. Laboratoire des Travaux Publics

Li S, Xu Q, Tang M, Iqbal J, Liu J, Xing Z, Liu F, Zhu D (2019) Characterizing the spatial distribution and fundamental controls of landslides in the three gorges reservoir area, China. Bull Eng Geol Environ 78:4275–4290. https://doi.org/10.1007/s10064-018-1404-5

Macfarlane DF (2009) Observations and predictions of the behaviour of large, slow moving landslides in schist, Clyde Dam reservoir, New Zealand. Eng Geol 109:5–15. https://doi.org/10.1016/j.enggeo.2009.02.005

Mahmut G, DrahorGokhan GO, KturklerMeric A, Berge T, Ozgur K (2006) Application of electrical resistivity tomography technique for investigation of landslides: a case from Turkey. Environ Geol 50:147–155. https://doi.org/10.1007/s00254-006-0194-4

Martha TR, Kerle N, Van Westen CJ, Jetten V, Kumar KV (2012) Object-oriented analysis of multi-temporal panchromatic images for creation of historical landslide inventories. ISPRS J Photogramm Remote Sens 67:105–119. https://doi.org/10.1016/j.isprsjprs.2011.11.004

Matsuura S, Asano S, Okamoto T (2008) Relationship between rain and/or meltwater, pore-water pressure and displacement of a reactivated landslide. EngGeol 101:49–59

Mondini AC, Guzzetti F, Reichenbach P, Rossi M, Cardinali M, Ardizzone F (2011) Semiautomatic recognition and mapping of rainfall induced shallow landslides using satellite optical images. Remote Sens Environ 115:1743–1757. https://doi.org/10.1016/j.rse.2011.03.006

Omowumi Falae P, Prasanna Kanungo D, Kumar Singh Chauhan P, Kumar Dash R (2019) Electrical resistivity tomography (ERT) based subsurface characterisation of Pakhi Landslide, Garhwal Himalayas, India. Environ Earth Sci 78:430. https://doi.org/10.1007/s12665-019-8430-x

ORGM (1996) Geological map of Azefoune at 1/50. 000scal, Publ. Serv. Géol. Algérie

Ouyang C, Zhao W, Xu Q, Peng D, Li W, Wang D, Zhou S, Hou S (2018) Failure mechanisms and characteristics of the 2016 catastrophic rockslide at Su village, Lishui, China. Landslides 15:1391–1400. https://doi.org/10.1007/s10346-018-0985-1

Perrone A, Lapenna V, Piscitelli S (2014) Electrical resistivity tomography technique for landslide investigation: a review. Earth Sci Rev 135(2014):65–82. https://doi.org/10.1016/j.earscirev.2014.04.002

Prokešová R, Kardoš M, Tábořík P, Medveďová A, Stacke V, Chudý F (2014) Kinematic behaviour of a large earthflow defined by surface displacement monitoring, DEM differencing, and ERT imaging. Geomorphology 224:86–101. https://doi.org/10.1016/j.geomorph.2014.06.029

Rybář J (2006) Climatic effects in the development of different types of slope movements Zprávy Geologického Výzkumu, 90–92

Su LJ, Hu KH, Zhang WF, Wang J, Lei Y, Zhang CL, Cui P, Alessandro P, Zheng QH (2017) Characteristics and triggering mechanism of Xinmo landslide on 24 June 2017 in Sichuan. China J Mt Sci 14(9):1689–1700. https://doi.org/10.1007/s11629-017-4609-3

Van Asch TWJ, Buma J, van Beek LPH (1999) A view on some hydrological triggering systems in landslides. Geomorphology 30:25–32

Varnes DJ (1978) Slope movements: type and processes. In: Eckel EB (ed) Landslides analysis and control. Transp Res Board Spec Rep 176:11–33

Wang J, Xiao L, Zhang J, Zhu Y (2019) Deformation characteristics and failure mechanisms of a rainfall-induced complex landslide in Wanzhou County, three Gorges Reservoir, China. Landslides. https://doi.org/10.1007/s10346-019-01317-1